

A Modified Hold Time Model for Total Flooding Fire Suppression

Abstract

This study analyzes the validity of theoretical models used to predict the duration (hold time) for which a halon-replacement suppression agent will remain within a protected enclosure. Two current models and one new formulation are investigated; the *sharp descending interface* model (as applied in NFPA 2001, Annex C), the *wide descending interface* model (implemented in ISO 14520.1, Annex E), and the *thick descending interface* model (introduced herein). These three models are validated through direct comparison to the data provided by a recent experimental study. Designed to characterize full scale agent draining dynamics, the experimental phase included 34 tests using seven different clean extinguishing agents (CEA).

Results show that the validity of the wide and sharp interface models is highly sensitive to the threshold of agent concentration decay being modeled; whereas the thick interface prediction method is not greatly susceptible to this input parameter. The thick interface model, while requiring one additional input parameter, allows for greater general agreement between the theory and experimental results while consistently providing conservative hold time predictions.

Keywords: NFPA 2001; ISO 14520; hold time; retention time; validation study; total flooding; clean agent

Introduction

Total flooding fire suppression systems deluge an enclosure with a gaseous suppressant such that combustion cannot be supported for an extended period of time. Systems consist of one or more pressurized fire suppressant storage vessels, a delivery pipe network, a discharge nozzle(s), and an adequately sealed, protected enclosure. Following system activation, the agent is allowed to flow to the nozzle and become dispersed throughout the design envelope. Typical applications include data processing and telecommunication facilities, museums, banks, clean rooms, and hospitals. The fire suppressant (agent), or clean extinguishing agent (CEA), is often required to remain within the protected enclosure for 10 minutes [1]. This duration is intended

to allow for arrival of manual fire suppression measures and cooling of potential sources of re-ignition. Systems are approved for installation only after sufficient evidence is provided to authorities that the minimum hold time requirement will be met. Design standards published by the National Fire Protection Association (NFPA) and the International Standards Organization (ISO) provide simplified physical models that predict any system’s hold time expectation. This is an evaluation of the time at which the agent concentration at a specified height falls to a specified concentration threshold. Although either design standard advocates nearly identical sets of model input data and methods for gathering this data the hold time prediction of the NFPA model is usually twice that of the ISO model¹. This difference deserves closer inspection, which is offered in this study.

Each theoretical model espouses a simplified assumption for species diffusivity, which results in different assumptions for agent distribution within the design enclosure. This assumption is responsible for the difference in hold time predictions and also each theoretical model’s name. The *sharp descending interface*, published in NFPA 2001, Annex C, assumes that the agent does not diffuse at all. ISO 14520.1, Annex E advocates the *wide descending interface*, which assumes that agent diffuses instantaneously in known proportions. In this study, the assumption taken for the dynamic agent distribution profile is reformulated as a piecewise combination of the *sharp* and *wide* theories. The proposed assumption, coined as the *thick descending interface* model, while requiring one additional input parameter, allows for greater general agreement between the theory and experimental results.

Theoretical Background

The sharp descending interface and the wide descending interface models combine well established theory on orifice flow and *worst case* assumptions to model the decay of CEA concentration as a function of time and elevation. Theoretical considerations and model construction are discussed elsewhere

¹This comparison is made for a typical height (75% of room height) and concentration threshold (85% of the initial discharge concentration). NFPA 2001 defines the hold time as the time when 85% of the initial discharge concentration remains [2] while Dewsbury & Whiteley, speaking about typical European practices under ISO 14520, propose a typical system expectation as 80% of the discharge concentration [3].

[1, 3, 4, 5, 6, 7, 8, 9].

Theoretical hold time models assume that the discharge process results in a homogeneous mix of CEA and air throughout the enclosure's volume. Previous studies have investigated the accuracy of this assumption via full-scale experimentation in semi-congested spaces aboard the decommissioned USS-SHADWELL [10, 11].

The bulk addition of gas species to the enclosure creates a risk of over-pressurization. As well, some modern CEAs vaporize as part of the discharge process. This consumes large amounts of latent energy and results in a drop in temperature and sometimes an under-pressurization risk. Discharge-related pressure transients are not considered in the hold time models as the hold time effectively does not begin until the discharge event ends. Consideration for the risk of enclosure implosion/explosion is available in the literature [12, 13, 14].

Thermal transients produced during agent discharge are not considered in the hold time models. Following discharge, the enclosure's contents are assumed to be at the same temperature as the gas surrounding the enclosure. In the present study's experimental phase, the resultant agent-air mixture was significantly colder than ambient conditions. This result is firstly due to expansion and/or vaporization processes that the agent is subject to during discharge. Secondly, this is due to no fires or other heat sources having been introduced during testing. This is consistent with total flooding design objectives, which call for rapid fire detection and system activation before the fire has become a significant threat (i.e. a large heat contributor).

Assuming the post discharge environment to be warmer than in actuality can result in an under-prediction of the agent draining rate. At the same time, the models assume that fresh air begins flowing into the design enclosure immediately following agent discharge, which is not consistent with actual conditions either. During the period of agent-air warming, directly following agent discharge, the agent-air mix gradually expands, thus not allowing the influx of fresh air into the enclosure during this period. The first condition serves to lengthen the predicted hold time duration while the latter results in shortened hold time predictions. It should be noted that excess agent is designed into the total flooding system to account for the agent mass that escapes the enclosure during the discharge event itself.

The sharp and wide interface models rely upon the *fan integrity* test to gather critical model input data. This is a non-invasive method for evaluating air tightness (or leakiness) of an enclosure. A calibrated fan is used to

pressurize or depressurize an enclosure. The resulting pressure change across enclosure boundaries and volumetric flow through the fan are used to measure the total amount of leakage area. Judicious treatment is given to the test method and uncertainty considerations in the literature [15, 16]. ISO and NFPA procedures vary slightly in how the results from fan inflow and outflow testing are averaged. These deviations, however, are nearly negligible in terms of overall model validity [4, 17].

Most agents available in the market have vapor densities greater than that of atmospheric air. Due to hydrostatic pressure differences between the agent-air mix and the gas surrounding the protected enclosure the agent will tend to drain out lower leakages while atmospheric air flows in through upper leakages. The magnitude of the pressure differential driving this agent draining process depends upon where the agent accumulates throughout the hold time. The fan integrity test measures the combined area of all leakages about enclosure boundaries but gives no knowledge of actual leak locations. The hold time models assume that leakages exist only in the compartment’s ceiling and floor but not in the surrounding walls. This results in the maximum possible hydrostatic pressure that drives agent draining. When the distribution of total leakage between upper and lower elevations is not known, it is assumed to exist, in half, at either elevation. This nominally provides a worst case scenario; allowing for the most rapid agent draining.

Figure 1 shows the agent concentration profiles in three hold time models considered in this study. The thick interface model is a newly proposed model developed in this study. The modified mathematical model is presented elsewhere while the present study seeks to validate the thick interface model and governing assumptions experimentally[5].

Assuming that gas species do not diffuse results in an infinitesimally thin interface between inflowing fresh air and the agent-air mix resulting after discharge. The wide interface model assumes that inflowing fresh air mixes instantaneously with the agent-air mixture to form a linear decay of agent concentration from the leading edge of the interface, H_i , to the uppermost elevation in the protected enclosure, H_0 . These two conditions represent theoretical extremes of a stratified model formulation. In this study gas diffusivity is formulated such that it provides a compromise between the sharp and wide models. The *thick descending interface* model assumes that the interface has a characteristic thickness across which the agent concentration is assumed to decay linearly. At time zero the interface does not exist. As fresh air begins to flow in it mixes with the top of the column of agent air,

forming a linear concentration decay through elevation. Given enough time, the interface grows to a maximum characteristic thickness and begins to descend towards the floor. When the leading edge of the interface reaches the floor’s elevation the interface gradually begins to decay in thickness. Eventually, the interface disappears, all agent has drained from the enclosure, and only fresh, atmospheric air remains.

The interface thickness arises from a balance between gravity and gas diffusion. The resulting agent profile from these forces is transient and forms a highly nonlinear interface between two gas species. The clean agent type, enclosure dimensions, enclosure obstacles, plumes above heat sources, and leaks located at various elevations in the walls pose too many unknowns. Given our current state of knowledge, a concise theoretical formulation for the characteristic thickness is not possible and as such, the characteristic thickness must be evaluated experimentally. After conducting 34 tests on 7 agent types, it is found that the characteristic thickness is a constant in time and also nominally has the same value for various agent types [5].

Experimental Background

All experiments are conducted in a 4.6 x 4.6 x 4.8 m (15 x 15 x 16 ft) high test enclosure. A schematic of the test bed is given in Figure 2. A series of 2.5 cm (1 in) diameter holes are drilled about the enclosure’s boundaries at 30 cm (1 ft) offsets from the floor and ceiling elevations. For each experiment dense rubber stoppers are added to or removed from these drill holes to control the total amount of upper and lower leakages provided for agent draining. The entire test bed and instrumentation design is modeled after the small scale prototypical work completed by Mowrer [8]. Extended documentation of the experimental setup and procedures is available in the literature [5].

Ambient pressure, temperature, and CEA volume concentrations are monitored inside the test enclosure at a series of elevations. This instrumentation layout parallels the theoretical hold time models in that they are resolved in two dimensions; temporally and spatially in the direction of gravity. The procedure for each experiment begins with a ‘fan integrity test,’ previously introduced. The fan integrity test is performed before and after each hold time test’s execution to ensure that the leakage configuration did not appreciably change during the period of agent discharge. Information gained from this test measure is used as input data to the theoretical models in making

hold time predictions.

The test enclosure is not thermally controlled although the relative humidity is dropped to approximately 40% before test initiation. Fires are not introduced in any experiments. The total flooding fire suppression system is manually activated and the CEA allowed to flow through a pipe network to a discharge nozzle inside the test enclosure. After agent discharge the enclosure is left undisturbed for a sufficient period of time to allow for observation of agent draining.

Throughout the agent draining phase, volume concentration measurements are monitored continuously and obtained at a series of points along a vertical axis within the enclosure. This data provides for direct interpretation of the experimental hold time, or the time at which a specified concentration exists at a specified height. Model validations presented in this study are only evaluated at the set elevations of operating instrumentation (no interpolation).

The Agent Distribution Profile

The agent distribution profile is the major differentiating factor between the three theoretical hold time models considered in this study. The applicability of each theoretical assumption can be ascertained through direct comparisons of the ideal and observed agent distribution profiles.

Figure 3 shows the observed agent distribution profile for each of the seven clean agents tested. The data set from a single, representative test for each agent is plotted. Each data series represents a single instant in time. The progress in time is depicted by lighter shades of gray in Figure 3. Data is presented in the elevation range for which gas sampling instrumentation is installed. At each plotted time step, the installation height for a given instrument and the agent concentration recorded at that instant is shown in Figure 3.

Figure 4 shows the ideal height-concentration relationship predicted by the models' considered in this study. Plotted data series represent an instantaneous *snapshot* in time where an advance in time is denoted by lighter shades of gray. Because Figures 3 and 4 share the same axes, direct, graphical comparisons between the observed and predicted agent distributions for various agent types can be made. In such a fashion, the validity of and limits of applicability for the sharp, wide, and thick modeled interface assumptions

can be observed.

Figures 3 and 4 show that the sharp interface model does not represent actual conditions. All agents have a distinguishable *thickness*; denoted by the change in elevation as a data trace spans from left to right (zero to full agent concentration). The wide interface model shows more reasonable agreement for agents IG-541 and IG-55 but predicts a far greater interface thickness than is observed for all other agent types. Figure 3 and 4 also show that the thick interface model developed in this study shows good agreement with experimental data for all agent types (except IG-100). However, the thick interface model relies on knowledge of the characteristic thickness. In this study, the experimental data is regressed with the objective of quantifying the observed characteristic thickness as a function of time and agent type.

It should be noted that agent IG-100 does not match any of the models. IG-100 is pure nitrogen, which has a vapor density less than that of atmospheric air. The agent gathers at lower elevations initially because the agent is cold (denser than air due to discharge and expansion) and then gathers at upper elevations as it thermally acclimates to the fresh air within the enclosure. IG-100 therefore does not show a stratified distribution and is not considered for further analysis in this study.

Figure 5 illustrates a method of assessing the time resolved interface thickness. HFC-23 experimental data is used as a sample case to analyze the thick interface model proposed in this work². The relationship between elevation and concentration is assumed to be linear. At each time step a linear regression is computed for all data points that exist within a concentration range of 15% to 85%³. Additionally, at each time step a linear regression is computed where at least 3 data points are available (no regression lines appear for the uppermost and lowermost data series).

The slope of the regressed line (hollow dotted lines),

$$\omega = \frac{(\Delta H/H_{max})}{(\Delta C/C_{max})}$$

is equal to the dimensionless interface thickness (when $\Delta C/C_{max} = 1$). This procedure is repeated at each data acquisition time step (5 second intervals

²This experiment's data is arbitrarily chosen for demonstration purposes in Figures 4, 5 and 6. The sharp interface model is used to predict a 13 minute hold time; indicating that this particular test is similar to typical total flooding systems in use today.

³This range of the concentration domain is arbitrarily chosen. It is observed in Figure 5 that data points lying in the shaded margins of the chart are not contributory data points when trying to linearly approximate the interface as a whole.

in this study) to determine the dependency of the interface thickness to time. Figure 6 shows the regressed dimensionless interface thickness as a function of the dimensionless time for the HFC-23 data set. Periodically, vertical jumps are observed as the regression is performed at sequential time steps due to the sampling probe entering (or exiting) the region of regressed data (in this case from 15% to 85% of the concentration scale). In general, the dimensionless interface thickness ranges between 0.15 and 0.25. This represents an interface thickness between 15% and 25% of the enclosure’s maximum height.

Figure 6 shows that the interface thickness is nominally constant in time.

A series of box plots are presented in Figure 7 that summarize all the experimental results. Each box plot is constructed from a population of data that includes the regressed characteristic thickness from each time step of a single experiment’s agent concentration data (ie. a single box plot in Figure 7 represents the entire set of plotted data values in Figure 6). Tests are grouped by agent type, which is labeled at the top of each section of Figure 7 with experimental the agent-air mixture density given below in units of kg.m^{-3} . Some experiments yield no characteristic thickness information because sufficient gas sampling instrumentation was not available. These experiments are not included in Figure 7; leaving a total of 26 charted data sets out of 34 conducted hold time tests.

Box plot construction does not assume that the data population is distributed in any predictable way. Rather, it serves to graphically describe the population in terms of the median value (red line inside box), lower and upper quartile values (lower and upper box bounding edges), the range wherein the majority of data values lie (black ‘whiskers’ extending 1.5 times the interquartile range above or below the box), and outlier data points, or the data plotted beyond the whiskers (red crosses)⁴. Because the population size is not described within the box plot it is included as a separate gray data trace on the rightmost y-axis.

The thickness of the interface is affected by many influences; inclusive of agent chemistry, buoyancy forces, diffusion forces, and turbulent mixing forces from thermal and mechanical sources, among others. As a general consensus, it is understood that the force of gravity will tend to stratify fluid mediums of disparate density while an increase in time can provide for

⁴The interquartile range (IQR) represents the population data values that are within the 2nd and 3rd quartiles. For example, the population {1,2,3,4,5,6,7,8} results in an IQR of 3 to 6.

prolonged interdiffusion and mixing between the two mediums. The counter-acting effects of these two parameters are analyzed by ordering the box plots in blocks by agent type (sectioned by black vertical lines) and by the respective test's duration (gauged by the predicted sharp interface hold time at 75% of maximum height, listed on the x-axis). Blocks of agent type progress from left to right in descending order of the agent-air mixture density (as given below the agent label in Figure 7). It is expected that interface thickness will follow an upward trend from left to right as the stratifying affect of gravity becomes less powerful for *lighter* agent types. Within each agent type division the individual tests' box plots are ordered from shortest to longest test duration. Here again, one tends to expect a trend of increasing interface thickness as test duration (or agent diffusion) advances.

The latter trend introduced above is not well supported by Figure 7. It is seen that from the densest agent at far left to the lightest agent at far right, there is not a reliable relationship of increased interface spreading (larger y-axis values) due to a lesser magnitude in the density difference between atmospheric air and the agent-air mixture.

The hypothesized, direct relationship between test time and increased interface spreading is identifiable for some but not all agent types. The agents HFC-125 and IG-55 demonstrate a broadening of the interface region (thickness of the interface) as test duration increases. HFC-23 shows constancy as test duration increases, and FK-5-1-12 and HFC-227ea demonstrate an unpredictable relationship between these two variables. For the typical range of interest (~ 10 minute hold times), HFC-125 demonstrates fairly constant interface thicknesses, which significantly increases as time is allowed to extend to 30 minutes and beyond. For the same range of interest, IG-55 is still exhibiting a dynamic relationship between test time and average interface thickness. The affect of assuming the thickness always equal to zero (sharp interface) or gradually spanning from a value of zero to two (wide interface) provides for greater modeling error in these same scenarios.

The agent IG-541 stands out due to the tightness of the interquartile range (box extents) and the observation that median value (red line) is different than that of any other test's data. A low level of confidence should be placed in this finding however due to the limited population size.

Figure 7 does not reveal an inverse relationship between the observed, characteristic thickness and the agent-air mixture vapor density as previously hypothesized. This possibility can be investigated further by regrouping the available data into categories by agent type alone. Figure 8 provides a new

series of box plots that regroup the data set of Figure 7 according only to agent type. Again however, there is little evidence to support the hypothesis that the characteristic thickness increases as agent molecular weight decreases (a variable that decreases from left to right).

The interquartile range (upper and lower box edges) for each agent type shown in Figure 8 overlaps the respective range of nearly every other agent type (with the exception of IG-541). This indicates that the data population represented by each box plot is probably not statistically different from one another. In order to derive an appropriate value of the characteristic thickness an average value must be obtained. The mean, standard deviation, and population size of each data set, categorized by agent type, is shown in Table 1. The final row in Table 1 represents metrics for the entire data population, regardless of agent type. It is found that the mean value of the characteristic interface thickness can be roughly represented as 0.25 ± 0.07 (or 25% of the maximum enclosure elevation $\pm 7\%$).

For the purposes of this study and eventual presentation of model validity this value is chosen to represent a characteristic interface thickness and is used as an input variable to the thick descending interface model; regardless of agent type or test duration.

Validation Results & Prediction Error

The validity of any of three hold time models considered in this study depends on the users understanding of what a *hold time* is. Previously, the hold time was defined as the duration required for the agent concentration to decay to a specified threshold at a specified elevation. Clearly, a user understanding the hold time to be 50% decay in agent concentration should expect the hold time at any given height to be longer than that for a 15% drop. NFPA 2001 requires that a minimum, 85%⁵ of the initial agent concentration must remain at the hold time (at the elevation of highest combustibles) [2]. ISO 14520 does not provide such guidance but does specify the applicable range of the model use to be 50% to 100% agent remaining at the hold time [18]. Regardless of what has been stated about model applicability, this study establishes new guidance based upon extensive, full scale, experimental evidence.

⁵Note that the theoretical construct of a ‘sharp interface’ as implemented in NFPA 2001’s sharp descending interface model is best understood as representing a 50% drop in agent concentration.

The predicted hold time is evaluated for differing concentration thresholds. Other researchers have failed to underscore the importance of this criterion, especially in that it is implicitly assumed as one half the initial value as used in formulating the sharp interface theory. By evaluating the experimental data using the exact same criteria as are input into the models for hold time predictions, a meaningful model validation is facilitated.

The hold time model is validated by comparing the theoretical and experimentally observed hold times as shown in Figure 9. In order to provide direct comparisons between experiments with various agent types, enclosure geometry, and differing amounts and distributions of leakages, the hold time is best expressed in dimensionless units⁶. Due to the flexibility allowed in the model user’s input hold time definition, three plots are provided; each assuming a different threshold for agent concentration. The elevation threshold at which the hold time is defined need not be incremented in the plots below as all elevations are simultaneously visualized (a dimensionless hold time value of 0 represents the hold time at the maximum elevation and a value of 1 represents the hold time at the minimum elevation).

A line of ‘exact correlation’ and dashed lines representing incremented error thresholds are included in each subplot of Figure 9. Data values on the line of exact correlation represent when experimental and theoretical hold times are equal. The error threshold lines represent percent deviations in the experimentally observed hold time values relative to the theoretical prediction. Data points lying below the line of perfect correlation represent a conservative condition where the experimental hold time duration is longer than the predicted value. Data values above this line represent a non-conservative scenario where the models predict an overly optimistic hold time.

All experimental hold time values are depicted three times in each plot; once for each of three hold time models under consideration. Plotted data points are colored by theory type and assume a marker shape based on agent type. The affect of agent type on model validity is difficult to discern. In general, no particular agent type can be observed to stand out from the others. This indicates that the clean agent type being modeled does not have a significant affect on model validity. On the other hand, the theoretical model used has a significant impact on model validity.

A significant portion of the data shown in Figure 9a lies in the non-

⁶Both experimental and theoretical values of the hold time are charted as the combined dimensionless quantity $(\beta \cdot \hat{t})$, which is presented in depth elsewhere [4, 5].

conservative region (above the 45° solid line). The newly introduced, thick descending interface model is shown to provide more accurate predictions of the hold time for a 15% drop in agent concentration than the other existing theories. Thick interface data points (black) populate the region of the axes between that of the sharp and wide theories. Hold times at lower left (measurements taken from upper elevations) are commonly one-and-a-half to two times the predicted value but as the interface descends to approximately one half of the enclosure height (advancing to the upper right) the data center at the line of exact correlation.

The thick interface was introduced as behaving like the wide interface as the thickness initially develops and then transferring to that of the sharp interface's descent once the characteristic thickness is met. This crossover in behavior is apparent in Figure 9a. Initially, the thick interface data overlaps that of the wide interface and eventually it is observed to populate a different region of the chart. This appears to occur at a dimensionless theoretical time of ~ 0.05 , which represents the interface passing an elevation of $\sim 85\%$ of maximum enclosure height.

The wide descending interface model (ISO 14520) results in experimental hold times that are up to 75% longer than the predicted values when the hold time is regarded as a 15% decay in concentration. This overly conservative trend is nominally constant through time or elevation as the interface descends. Overly conservative hold time predictions result in an inability of system designers to accurately justify whether a 10 minute hold time can be met. This problem persists in practice even when many total flooding system designs can easily meet and surpass the hold time requirement established by the Authority Having Jurisdiction (AHJ). When over-designed systems can not be achieved, this situation can potentially lead to devaluing due to inaccurate model use.

Figure 9b assumes the hold time to represent a 50% decay in agent concentration. Because each of the three theories model this concentration threshold equally, most data points directly overlap one another. ISO and NFPA standards adopt slightly different values of the vapor density of agents, the density of atmospheric air, and methods of measuring the amount of leakage present in an existing structure. Due to this, slight jitter is observed between wide and thick data points. In Figure 9b, the thick interface model is computed using the same assumptions as the sharp interface model; thus, perfectly overlapping all of the wide interface data points (no red data visible).

Figure 9c assumes the hold time to represent an 85% decay of the initial

agent concentration or, in other words, only 15% of the total agent remains in the enclosure. From an industrial application, an 85% decay of agent is usually not applicable. However, hold time results are presented in this case as well to demonstrate the versatility of the thick descending interface model. In Figure 9c, the plotted theoretical hold time values of the sharp and wide theories are the same as those in Figure 9b. Either of these existing theories do not support a 15% agent remaining input value and therefore are not meant to be applicable in this range.

Table 2 provides supplemental quantitative measures of model validity. Each data value presented in Figures 9a, b and c is first computed as an error level relative to the theoretical prediction and then summarized in three quantities; the mean, cubic mean, and standard deviation. The mean and standard deviation should be fairly intuitive to the reader and the cubic mean can be understood to represent an always-positive metric for the total deviation of all experimental hold times from the theoretical predictions.

The third column of Table 2, where the hold time represents a 15% decay in agent concentration, is most relevant to a typical design scenario. In the sharp interface theory, actual hold times can be roughly $13\% \pm 14\%$ shorter than predicted values with a total average error of 19%. This justifies the graphical observation in Figure 9a where most data points lie above the 45° solid line.

The thick interface model tends to provide more accurate hold time predictions than the wide interface model if similar metrics are considered. Both theories provide predictions that are typically conservative (mean error is positive) even when considering a single standard deviation difference from this mean value. The thick interface model presented in this study provides hold time predictions that are significantly less conservative than that of the wide interface theory however. Experimental hold times are longer than thick interface model predictions by $31\% \pm 28\%$ as compared to $56\% \pm 24\%$ for wide interface model predictions. It is interesting to note as well that the thick interface models agent draining with increasing accuracy as the agent concentration threshold is set lower (moving from left to rightmost column in Table 2).

Conclusions

This study questions the validity of two prevalent models used to predict the duration for which a modern, halon-replacement agent will remain within a protected enclosure. A novel model formulation is introduced and shown to provide more accurate predictions of agent draining dynamics than either of the existing methods. The results of a recent experimental campaign including seven common clean agent varieties and 34 full scale tests are used to assess model validity.

The applicability of a single differentiating factor between the three considered models - the profile of agent distribution through elevation - is investigated. The assumption taken for this concentration profile constitutes a titular basis for each considered model. The sharp interface model assumes that fresh air and agent stratify across an infinitesimally thin interface (published in NFPA 2001). The wide interface model assumes a linear concentration gradient across the air-agent interface width, which has a thickness that ultimately spans the total height of the design enclosure (published in ISO 14520). The modified model formulation, proposed as the *thick descending interface* model assumes an interface of known thickness. This constitutes an additional input parameter, the *characteristic thickness*, ω , which is extracted from the experimental data by linear regression for use in this study.

Within this study, and typical to the industry, the hold time is defined as the duration required for the agent concentration to decay 15% of its initial value at a set elevation within the design enclosure. Experimentally observed hold times at elevations between 95% and 40% of total enclosure height are generally longer than the thick interface model predictions by $\sim 30\%$. These same values are longer than the wide interface by $\sim 60\%$ and shorter than the sharp interface theory by $\sim 10\%$. The last of these findings is a cause for alarm in that the sharp interface model is providing non-conservative hold time predictions.

Acknowledgments

This research effort was begun under the auspices of the NFPA 2001 Technical Committee on Gaseous Fire Extinguishing Systems. Experimental work was made possible in thanks to the generous donations of suppressant agents, system hardware, system design specifications, and technical representatives

of 3M Company, Ansul Incorporated, Chemetron Fire Systems, Fike Corporation, Kidde-Fenwal Incorporated. Standardization of testing was largely facilitated by Fike Corporation, which provided a modern test facility and multiple technicians. Gas sampling instrumentation was provided by 3M Company, Ansul Incorporated, Chemetron Fire Systems, DuPont Fluoroproducts, Fike Corporation, and Sevo Systems. Equipment for and execution of all door fan integrity testing was provided by Retrotec Incorporated.

The authors' appreciation for the keen foresight and efficiency of attendees to the test phase is gratefully recognized. Contributing members of the research team include Dale Edlebeck, Colin Genge, Eric Haberichter, Howard Hammel, Gene Hill, Daniel Hubert, Dai Heming, Jim Marquedant, Mark McLelland, Richard Niemann, John Schaefer, Seth Sienkiewicz, Brad Stilwell, and Bob Whiteley.

Without the encouragement and assistance of Paul Rivers this study would not have been realized. The extended efforts of Michael Barrera and John Woycheese in the first year allowed for the success this project has found today.

Discussions with faculty and fellow students at Worcester Polytechnic Institute are graciously acknowledged.

References

- [1] Dewsbury, J. and Whiteley, R.A. "Extensions to standard hold time calculations," Fire Technology, Vol. 36, No. 4, pp. 267-278, Nov. 2000.
- [2] "NFPA 2001: Standard on clean agent fire extinguishing systems," National Fire Protection Association, Quincy, MA, Annex C, 2008.
- [3] Dewsbury, J., and Whiteley, R.A. "Review of fan integrity testing and hold time standards," Fire Technology, Vol. 36, No. 4, pp. 249-265, Nov. 2000.
- [4] Hetrick, T. "Analysis of hold time models for total flooding clean extinguishing agents," Fire Technology, Vol. 44, No. 3, pp. 239-261, Sept. 2008.
- [5] Hetrick, T. "Development and Validation of a Modified Clean Agent Draining Model for Total Flooding Fire Suppression Systems," M.S. thesis, Worcester Polytechnic Institute, Worcester, MA, 2008.

- [6] Saum, D., Saum, A., Messing, M. and Hupman, J. "Pressurization air leakage testing for Halon 1301 enclosures," Substitutes and Alternatives to Chlorofluorocarbons and Halons, Washington, D.C., 1988.
- [7] DiNenno, P.J., and Forssell, E.W. "Evaluation of the door fan pressurization leakage test method applied to Halon 1301 total flooding systems," Journal of Fire Protection Engineering, Vol. 1, No. 4, pp. 131-140, 1989.
- [8] Mowrer, F. "Analysis of vapor density effects on hold times for total flooding clean extinguishing agents," Halon Options Technical Working Conference, 16th Proceedings, Albuquerque, NM, pp. 1-12, May 2006.
- [9] O'Rourke, S.T. "Analysis of hold times for gaseous fire suppression agents in total flooding applications," M.S. thesis, University of Maryland, College Park, MD, 2005.
- [10] Black, B., Maranghides, A., Sheinson, R., Peatross, M., and Smith, W. "Real scale halon replacement testing aboard the ex-USS Shadwell: post fire suppression compartment characterization," Halon Options Technical Working Conference, 6th Proceedings, Albuquerque, NM, pp. 1-12, May 1996.
- [11] Maranghides, A., Black, B., Sheinson, R., Friderichs, T., and Peatross, M. "Discharge system modifications: real scale halon 1301 replacement testing," Halon Options Technical Working Conference, 6th Proceedings, Albuquerque, NM, pp. 1-12, May 1996.
- [12] Genge, C. "Preventing excessive enclosure pressures during clean agent discharges," Halon Options Technical Working Conference, 15th Proceedings, Albuquerque, NM, pp. 1-16, May, 2005.
- [13] Harry, L., Meltzer, J., Robin, M. "Development of room pressure in the discharge of FM-200 compared to the strength of various structural components," Halon Options Technical Working Conference, 7th Proceedings, Albuquerque, NM, pp. 1-12, May, 1997.
- [14] Robin, M., Forssell, E., and Sharma, V. "Pressure dynamics of clean agent discharges," Halon Options Technical Working Conference, 15th Proceedings, Albuquerque, NM, pp. 1-11, May, 2005.

- [15] Sherman, M., Palmiter, L. “Uncertainties in fan pressurization measurements,” Airflow Performance of Building Envelopes, Components and Systems, ASTM STP 1255, American Society for Testing and Materials, Philadelphia, PA, pp. 266-283, 1995.
- [16] Sherman, M. “The use of blower-door data,” Indoor Air, Vol. 5, Issue 3, pp. 215-224, 1995.
- [17] Hetrick, T., Rangwala, A. “Analysis of hold time models for total flooding clean extinguishing agents,” Fire Suppression and Detection Research and Applications - A Technical Working Conference (SUPDET 2008), Orlando, FL, March, 2008.
- [18] “ISO 14520-1: Gaseous fire extinguishing systems - physical properties and system design - part 1: general requirements,” International Standards Organization, Geneva, Switzerland, Annex E, 2006.

List of Figure Captions

1. Concentration distribution of agents in the sharp and wide interface models. The thick interface model is a new model proposed in this study. The thickness of the interface is estimated from test data of 34 full scale tests.
2. Schematic of the test bed. Ambient pressure probes and controllable leakage areas are shown. Temperature and gas sampling probes (not shown) are located 60 cm (2 ft) east of the central axis.
3. Typical observed agent distribution profiles.
4. Theoretical agent distribution profiles.
5. Diagram of interface thickness analysis procedure.
6. Dimensionless interface thickness versus dimensionless time. It is observed that the characteristic thickness is relatively constant as the agent drains out of the enclosure. The nondimensionalization is discussed elsewhere [5].
7. Results of the dimensionless experimental interface thickness regression. Each section of the chart represents a single agent type, which are ordered from left to right according to decreasing magnitude of the agent-air mixture density, ρ_{mix} , given in $\text{kg}\cdot\text{m}^{-3}$. Population sizes for each summary box plot are in gray on the rightmost y-axis.
8. Box plots summarizing the dimensionless experimental interface thickness regression data as categorized by clean agent type. Each section of the chart represents a single agent type that is ordered from left to right according to decreasing magnitude of the agent-air mixture density relative to that of atmospheric air (buoyant driving force of agent draining). Population sizes for each summary box plot are in gray on the rightmost y-axis.
9. Validation plots of the dimensionless theoretical hold time versus the dimensionless experimental hold time for a 15%, 50% and 85% decay in agent concentration. Plotted values are calculated as the quantity $(\beta \cdot t)$. Error lines represent percent deviations from the theoretical hold time prediction.

List of Table Captions

1. Summary Values of the Regressed Dimensionless Interface Width
2. Quantitative Summary of Experimental Error Relative to the Theoretical Prediction

Table 1: Summary Values of the Regressed Dimensionless Interface Width

Agent Type	Mean Value	Standard Deviation	Population [# data points]
FK-5-1-12	0.22	0.06	192
HFC-125	0.27	0.08	1187
HFC-227 _{ea}	0.24	0.06	1451
HFC-23	0.20	0.03	1032
IG-541	0.42	0.02	67
IG-55	0.26	0.06	1190
All Agents	0.25	0.07	5119

Table 2: Quantitative Summary of Experimental Error Relative to the Theoretical Prediction

Quantitative Measure	Theory Type	Concentration Decay at the Hold Time		
		15%	50%	85%
Cubic Mean (Percent Error)	Sharp Interface	19%	27%	99%
	Wide Interface	61%	28%	99%
	Thick Interface	42%	27%	24%
Mean (Percent Error)	Sharp Interface	-13%	20%	76%
	Wide Interface	56%	20%	77%
	Thick Interface	31%	20%	16%
Standard Deviation (Percent Error)	Sharp Interface	14%	19%	63%
	Wide Interface	24%	19%	63%
	Thick Interface	28%	19%	18%

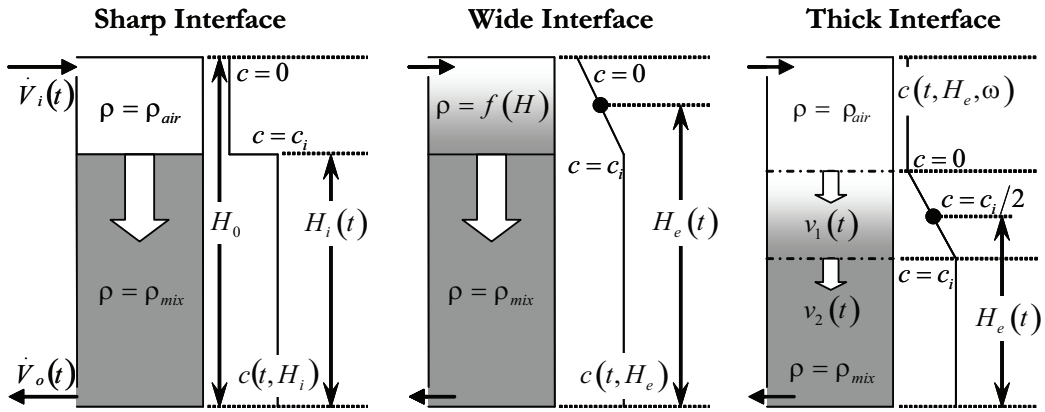


Figure 1: Concentration distribution of agents in the sharp and wide interface models. The thick interface model is a new model proposed in this study. The thickness of the interface is estimated from test data of 34 full scale tests.

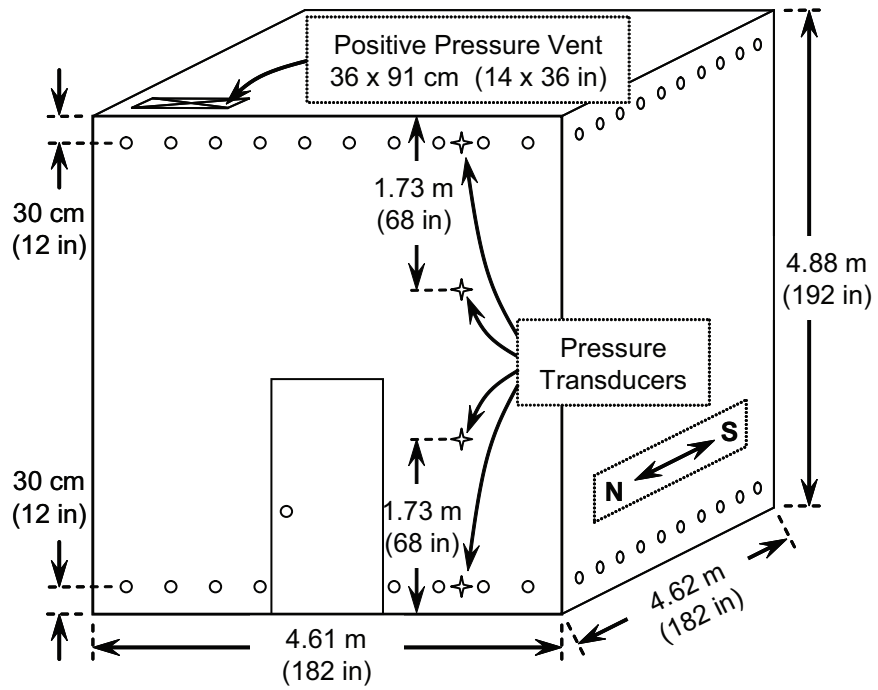


Figure 2: Schematic of the test bed. Ambient pressure probes and controllable leakage areas are shown. Temperature and gas sampling probes (not shown) are located 60 cm (2 ft) east of the central axis.

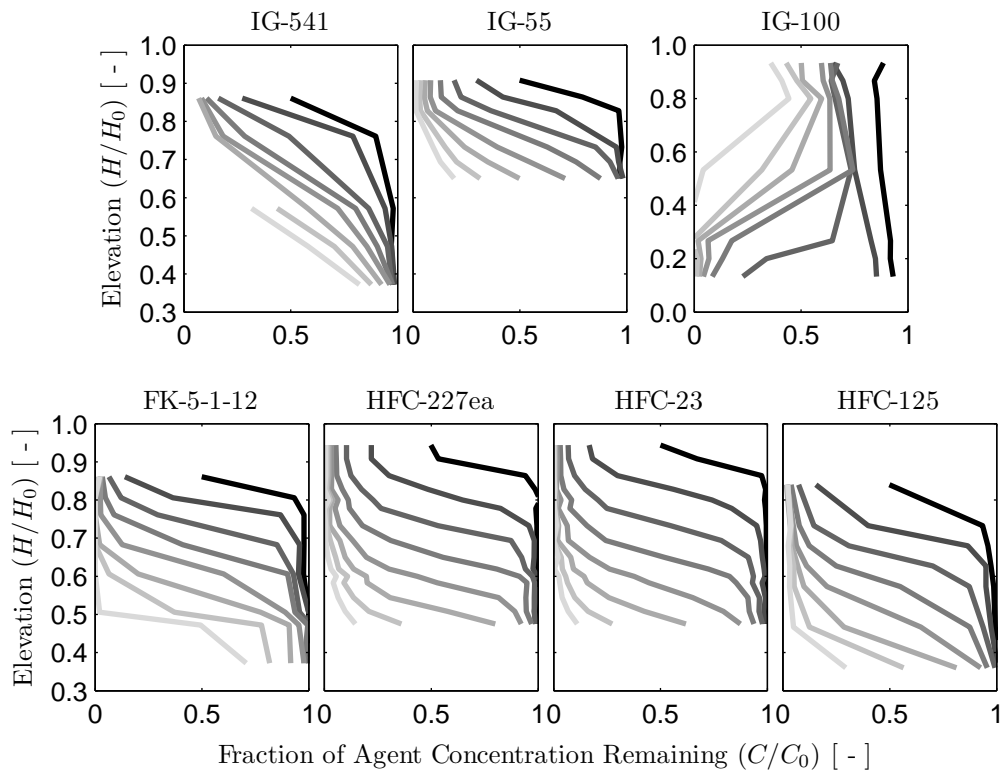


Figure 3: Typical observed agent distribution profiles.

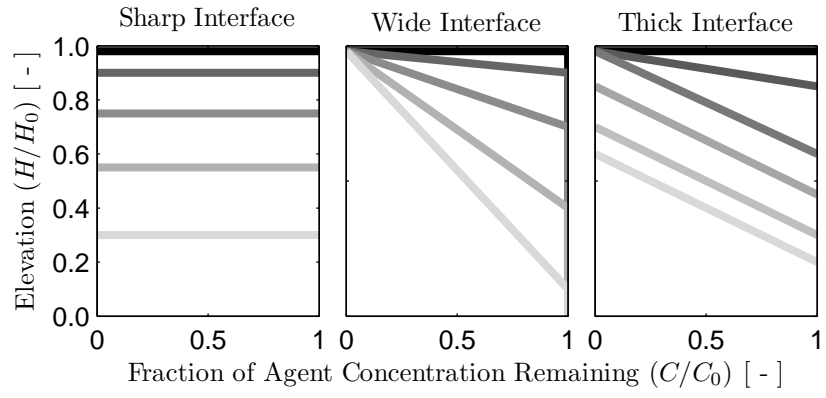


Figure 4: Theoretical agent distribution profiles.

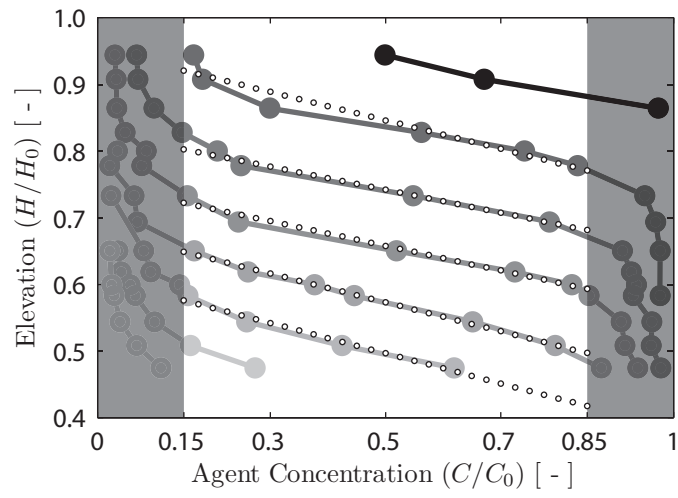


Figure 5: Diagram of interface thickness analysis procedure.

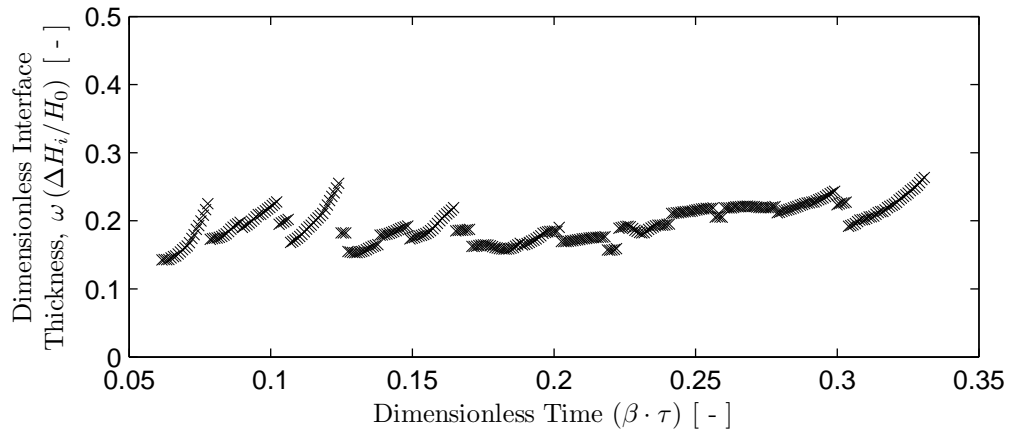


Figure 6: Dimensionless interface thickness versus dimensionless time. It is observed that the characteristic thickness is relatively constant as the agent drains out of the enclosure. The nondimensionalization is discussed elsewhere [5].

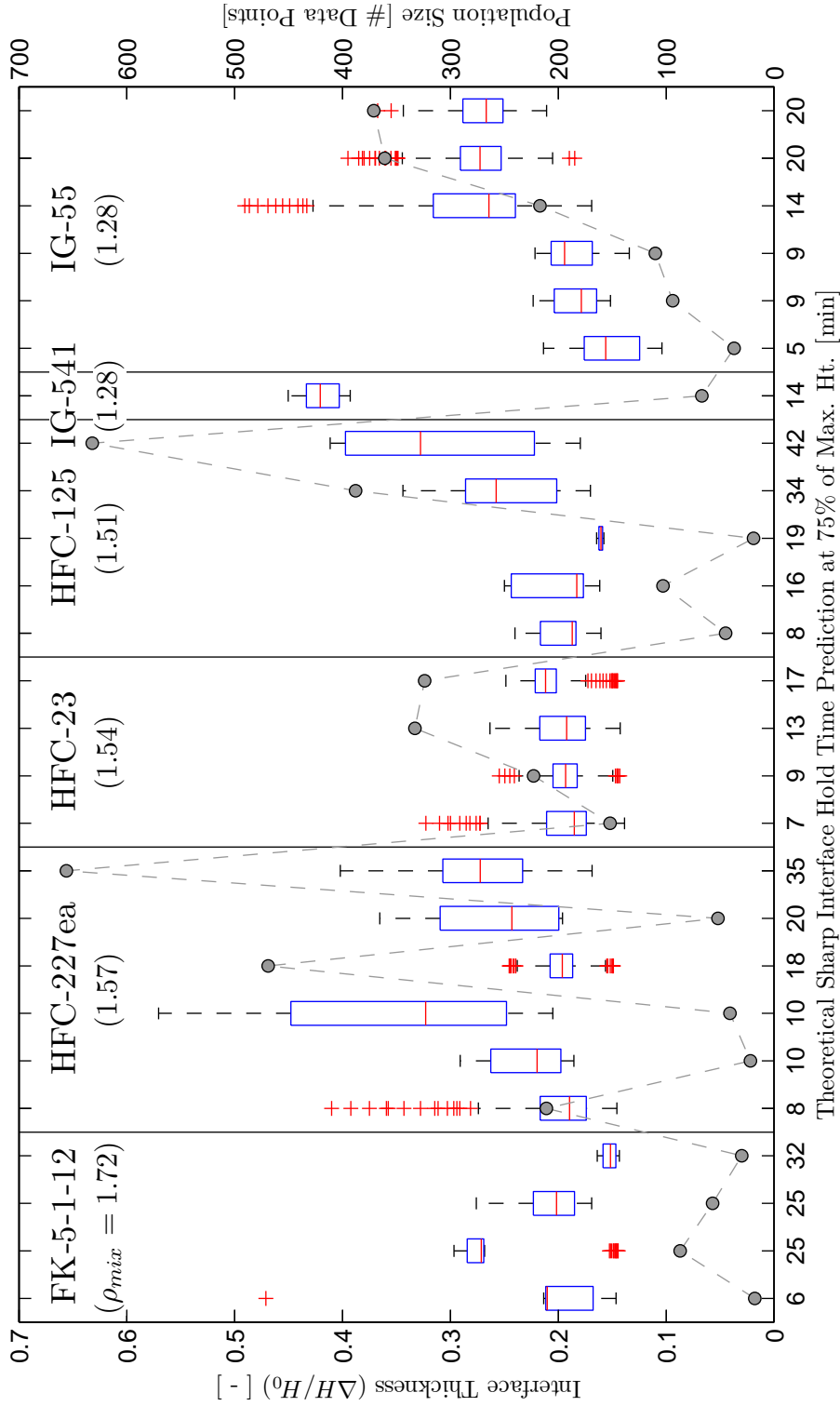


Figure 7: Results of the dimensionless experimental interface thickness regression. Each section of the chart represents a single agent type, which are ordered from left to right according to decreasing magnitude of the agent-air mixture density, ρ_{mix} , given in $\text{kg}\cdot\text{m}^{-3}$. Population sizes for each summary box plot are in gray on the rightmost y-axis.

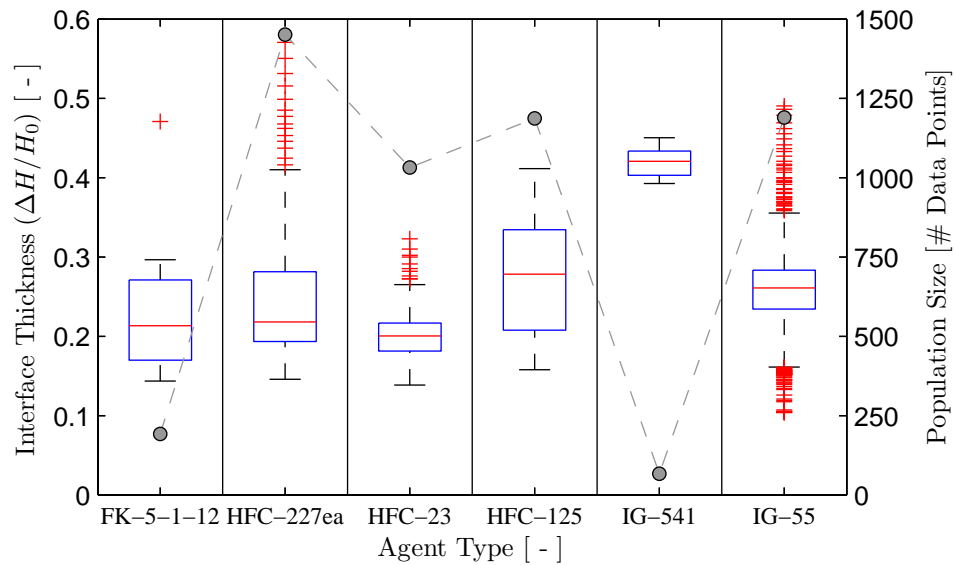


Figure 8: Box plots summarizing the dimensionless experimental interface thickness regression data as categorized by clean agent type. Each section of the chart represents a single agent type that is ordered from left to right according to decreasing magnitude of the agent-air mixture density relative to that of atmospheric air (buoyant driving force of agent draining). Population sizes for each summary box plot are in gray on the rightmost y-axis.

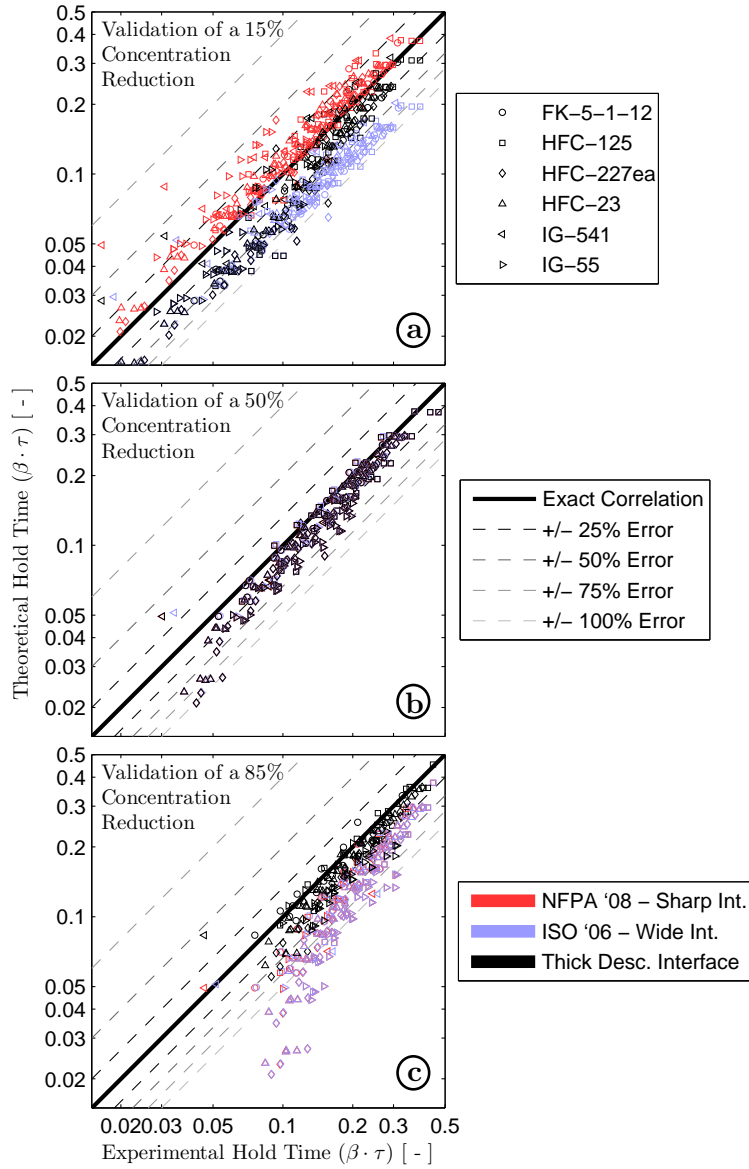


Figure 9: Validation plots of the dimensionless theoretical hold time versus the dimensionless experimental hold time for a 15%, 50% and 85% decay in agent concentration. Plotted values are calculated as the quantity $(\beta \cdot \hat{t})$. Error lines represent percent deviations from the theoretical hold time prediction.